Eur. Phys. J. A (2024) 60:142
https://doi.org/10.1140/epja/s10050-024-01353-z

THE EUROPEAN PHYSICAL JOURNAL A

Regular Article - Experimental Physics

Effects of shape/phase transition regions on neutron capture cross sections

A. Couture[1,a], **R. B. Cakirli**[2,3], **R. F. Casten**[4]

[1] Los Alamos National Laboratory, Los Alamos, New Mexico 87545, USA
[2] Department of Physics, Istanbul University, Istanbul 34134, Turkey
[3] Max-Planck-Institut für Kernphysik, Saupfercheckweg 1, D-69117 Heidelberg, Germany
[4] Wright Lab, Yale University, New Haven, CT 06520, USA

Received: 7 March 2024 / Accepted: 29 May 2024

Communicated by Wolfram Korten

Abstract A recent study found a new, purely empirical correlation between two-neutron separation energies and neutron capture cross sections in keV neutron energy regimes. In shape/phase transition regimes, such as that near A= 150, S_{2n} values show an anomaly—a flattening of the normal near linear decrease with neutron number. This paper addresses two questions: (1) Using this new correlation, is this anomaly in S_{2n} values sizeable enough to produce an observable effect in capture cross sections? and (2) Can the correlation be used to quantitatively reproduce the cross sections in the transition region? It is found that the answer to both questions is in the affirmative. Possible relations to the *r*-process are briefly discussed.

1 Introduction

Recently, an advance in quantitatively linking S_{2n} values with neutron capture cross sections has been the discovery of a new, purely empirical, correlation between neutron capture cross sections at neutron energies relevant for nucleosynthesis and two-neutron separation energies, S_{2n} [1,2]. We refer to Ref. [2] below as CCC21. In Ref. [2], a simple exponential fit function (given below in Eq. 1) was developed to describe this correlation. Figure 1 illustrates this correlation for one mass region. Figure 1 (top) shows the S_{2n} values for nuclei from Nd through W in the $N = 84-112$ rare earth region [3]. It shows that a clear deviation from linearity in S_{2n} occurs in the shape/phase transition region near $A = 150$, for N from 88 to 92 where the S_{2n} values plateau for the nuclei Nd to Dy. This is well understood as due to an increase in binding, relative to the downward trend, as these nuclei evolve from spherical to prolate deformed (see, for example Ref. [4]). Figure 1 (middle) shows the correlation between S_{2n} values and neutron capture cross sections at 30 keV for this region. The capture cross sections are the 30 keV Maxwellian averaged cross sections (MACS) taken from Ref. [5]. Note that the S_{2n} values in the plot for capture on a nucleus (Z, N) are for $(Z, N+2)$ as discussed in Ref. [1]. Figure 1 (bottom) shows a comparison of the measured 30 keV MACS cross sections and those calculated with the experimental S_{2n}(N+2) values using Eq. 1.

The correlation is striking, extending over a range of cross sections that spans an order of magnitude. We will discuss this further below. For now we note, as shown briefly in Ref. [1] and in considerable detail in Ref. [2], the same correlation persists for all neutron energies in the range from $kT = 5 - 100$ keV and for almost all non-magic nuclei above A∼110 [2].

The purpose of this paper is to carry out a specific test to see if this correlation is sensitive enough to imply significant changes in neutron capture cross sections due to anomalies in S_{2n} and if our correlation could be exploited to accurately reproduce capture cross sections in such regions. To do this we choose a region near stability, with well-known S_{2n} values and neutron capture cross sections, as a test bench.

While this region centers on stable nuclei with known neutron capture cross sections, the present results can provide an indication of what might happen in newly found regions of S_{2n} anomalies where the capture cross sections are unknown. In such regions, cross section estimates currently rely on Hauser-Feshbach theory, but are difficult to determine reliably [6,7].

Notably, though the test region is far from the locus of the *r*-process, such a test could provide a useful indication of what may be expected in a shape-changing region fur-

[a] e-mail: acouture@lanl.gov (corresponding author)

Published online: 02 July 2024

ther from stability where *r*-process nucleosynthesis is taking place.

2 Methods and results

We proceed in a very simple way. Knowing the S_{2n}-cross section correlation in this mass region and a fit function that describes it, we simply plot the cross sections predicted by it for the experimentally measured S_{2n} values and compare those to what would have been obtained by the same fit function if we substitute a linear dependence of S_{2n} for nuclei between N=86 and N=96. For the fit correlation function we use the expression shown in Eq. (1) from Ref. [2] (updated from Ref. [1]).

$$\sigma_{fit} = p_0 \cdot e^{p_1 \cdot (S_{2n} + p_2)} \tag{1}$$

where p_0 is 0.0106±0.0005, p_1 is 0.7644±0.0035 and p_2 is zero for even-even deformed nuclei in the rare earth region. For transitional even-even nuclei in the rare earth region $p_2 = -1.92$ [2]. Note that these values were obtained earlier in CCC21 for entire regions of nuclei and are not fit to the specific nuclei discussed in this paper. The results, shown for Gd (those for Nd and Sm are similar) in Fig. 2 (left), are striking. Note that there is a large difference in the predicted cross sections. It amounts to ∼500 mb in the actual transition region between N= 88 and 90 and the reductions in cross sections there, relative to those obtained for the actual S_{2n} values, are 35–50%. That is, the non-linearity in S_{2n} changes the neutron capture cross sections by as much as a factor of two.

The remarkable agreement seen in Fig. 1(bottom), and noted earlier, extends, in particular, to the roll-over in cross sections for Gd and Sm near $N = 90$ in comparison to the smooth behavior of other nuclei in regions without anomalies in S_{2n}.

2.1 Comparison with TALYS calculations

A related issue is whether this effect would be visible or impactful if considered in the framework of another method to calculate cross sections generally and MACS in particular. We chose to compare to the TALYS reaction model code as it is extensively documented and freely available [8]. Shown in the middle panel of Fig. 2 is a comparison of the CCC21 fit function, TALYS, and the experimental MACS 30 keV

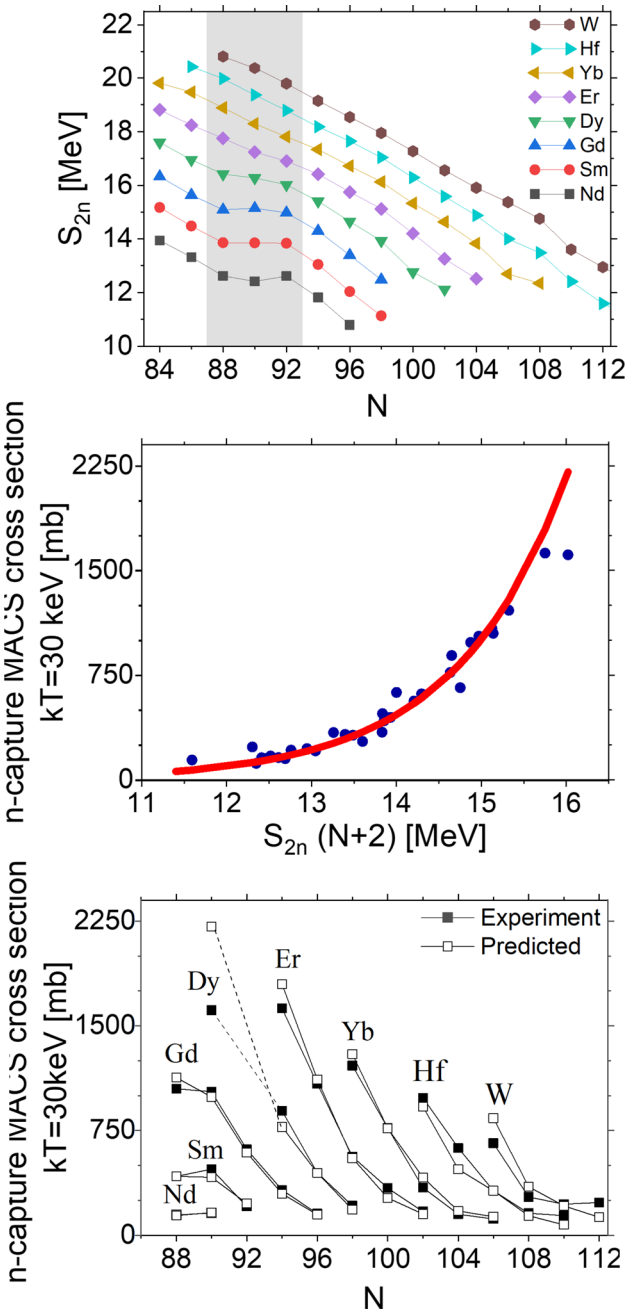

Fig. 1 (Top): The S_{2n} values from Nd to W in the $N = 84-112$ region [3]. The neutron numbers corresponding to the phase/shape transition in Nd-Dy are shaded. (Middle): Experimental neutron capture MACS cross sections at 30 keV [2] versus S_{2n}(N+2) values [3] and a corresponding fit using Eq. 1. (Bottom): Experimental and predicted neutron capture MACS cross sections at 30 keV [5] against neutron number for even–even nuclei from Nd through W. The neutron capture cross section of ^{158}Dy has not been measured [5]. For this reason, the ^{156}Dy and ^{160}Dy data points are connected with dashed lines

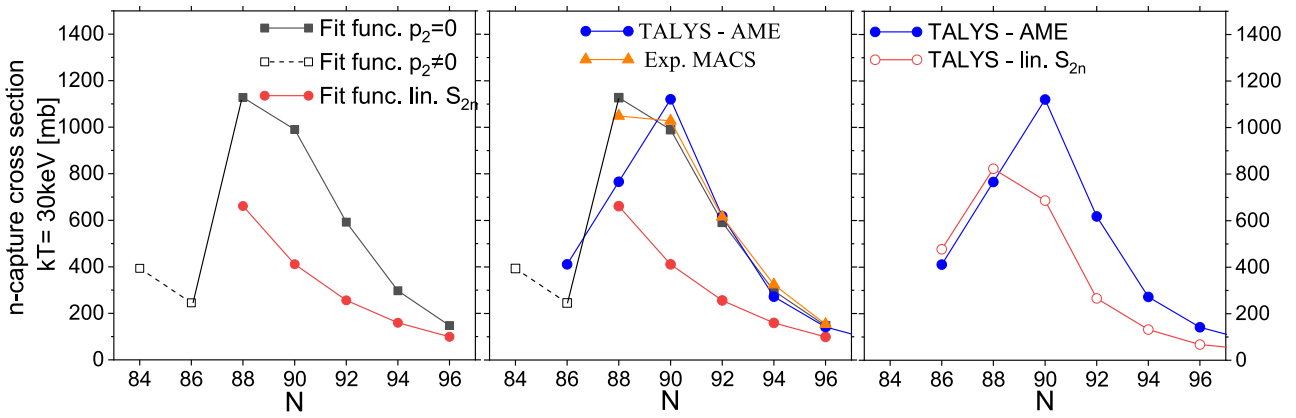

Fig. 2 (Left): Comparison of predicted 30 keV MACS neutron capture cross sections in the even Gd isotopes, based on the S_{2n}-σ(N) correlation reported in Ref. [2], for two sets of S_{2n} values: the experimental values (black), and those that would be obtained with a linear interpolation of S_{2n} in Fig. 1 from $N = 86 - 96$ (red). The value p_2=0 is used for the deformed and transitional rare earth nuclei, with N$\geq$ 88, while $p_2\neq0$ is used for N<88. (Middle): In addition to the left panel, experimental MACS and TALYS calculations using the AME mass values [3] are shown. (Right): Comparison of the TALYS-AME calculations (same as the middle panel) with TALYS results using masses obtained by linearizing S_{2n} values in the shape transition region. The mass excess values that give the linear function in S_{2n} were changed manually in the TALYS program (see text for further details)

kT cross sections [5]. For TALYS, the values are based on the default TALYS parameters. TALYS shows a clear deviation relative to the measured cross sections for N=88, but largely reproduces the remaining cross section values. We also performed TALYS calculations using the "best" parameter option. The largest impact compared to the default calculations was at N=88, where the "best" parameter option brought the TALYS result more in line with the measured value. However, since the parameters are individually tuned nucleus by nucleus, they were not available in Gd isotopes outside of $88 \leq N \leq 96$. Thus, this approach lacks predictive capability. As such, we focus the rest of our discussion on trends shown in TALYS default calculations.

For the CCC21 parameterization, linearizing S_{2n} allowed a straightforward way to estimate the effect of removing a known phase transitions. With TALYS, a slightly different, but equivalent, approach is needed since TALYS uses single neutron separation energies and mass excesses. Thus, we linearized S_{2n}, over the same range of neutron numbers, now including the odd neutron number nuclei. We used these values to determine mass excesses needed by TALYS to obtain results applicable in the absence of the phase/shape transition. The results of this are shown in the right panel of Fig. 2.

There are several features to note. One, as expected, the change reduces the calculated cross section for $N > 88$. Two, the overall shape is largely unchanged, and is broadly similar to the result of removing the phase transition in the calculations with the CCC21 predictions (seen in the left and center panels of Fig. 2). The absolute magnitude of the change using a linearized S_{2n} is initially somewhat larger in the case of the CCC21 calculations, while the cross sections reach similar or even smaller levels in CCC21 by the time one reaches N=96. Further, the cross section evolution in CCC21 falls more smoothly than that seen in the default TALYS calculations. This indicates that, while the CCC21 parametrization relies on nuclear mass changes, the phase transition is enforced in a more complex way in the TALYS representation. More simply, our correlation requires less input experimental information (masses) than TALYS.

3 Discussion

The comparison above was developed in a region of the chart of nuclei where the experimental basis is largely complete, with rich information on structure and reactions on the nuclei of interest. In contrast, in an r-process environment, the available structural data will be largely absent, with perhaps only mass measurements to guide calculations. As such, a more transparent, simple approach like CCC21 that directly translates mass information into capture cross section predictions may offer increased predictive power for such cross sections in regions where new phase transitions may be observed in the future.

3.1 Potential astrophysical implications

It has long been recognized that nuclear structure is intimately involved, and its effects are observed, in the synthesis of the chemical elements in astrophysical environments. Early seminal works recognized the transition from charged particle fusion to neutron induced reactions that was observed

at the sudden abundance drop at the iron peak [9,10]. Heavy element peaks in regions of neutron capture nucleosynthesis were tied directly to neutron shell closures (see e.g. [9–12]).

For the rapid neutron capture process, much of the buildup of heavy elements takes place under conditions of nuclear statistical equilibrium (NSE), where the environment is hot enough that the photon bath allows photodissociation to compete with neutron capture. More precisely, neutron capture proceeds on a single elemental chain (Z) towards progressively lower neutron separation energy until the photon energy and density allows (γ, n) reactions to become competitive with further neutron capture, a very steep function of S_n. Once $(\gamma, n) \longleftrightarrow (n, \gamma)$ equilibrium is achieved, further neutron capture is inhibited until β-decay takes place. Decay moves the nucleus to higher Z and lower N, consequently moving to larger S_n; the process again continues.

In effect, the temperature sets a photon energy and density, which in turn sets an S_n at which the $(\gamma, n) \longleftrightarrow (n, \gamma)$ equilibrium will be achieved.

As a result, NSE nucleosynthesis proceeds almost exclusively at an S_n value fixed by the temperature, and the primary nuclear physics inputs needed to define the r-process path during NSE are the nuclear masses (from which S_n is derived) and the β-decay lifetimes [13–17]. As many authors have discussed, anomalies in the normally smooth behaviour of S_n arising from nuclear structure changes, like sudden shape changes, will give rise to changes in the r-process nucleosynthesis path if the structure change takes place in nuclei near the r-process path or if the S_n shift propagates to much higher N. Similar effects can also shift the positions of the r-process abundance peaks due to changes in shell closures. Notably, Surman and collaborators showed that the rise of the rare-earth peak in the r-process abundance distribution came from exactly this type of S_n anomaly, or "kink", as they described it [15].

Subsequently, it has been observed that while NSE conditions are important for the majority of the build-up of the heavy elements in the r-process, after falling out of NSE, there can still be an adequate neutron exposure (population of free neutrons) to shift abundances; in this case, individual neutron capture cross sections play an enhanced role [7,18–20]. Depending on the astrophysical environment, different effects can give rise to the neutron exposure. It could be a "cold" r-process, such as is postulated in the tidal outflow from a neutron star merger, where the rapid cooling results in a relatively high neutron:seed ratio at fallout from NSE. It could be driven by β-delayed neutron emission in the β-decay towards stability post freeze-out from a traditional "hot" r-process. Regardless of its origin, the critical conditions are that there is a significant neutron exposure to drive rapid neutron capture and the temperature is sufficiently low that the photon energy is too low to drive photodissociation at the dominant S_n.

Under these conditions, individual neutron capture cross sections once again play a critical role in the determination of the abundances of the r-process nucleosynthesis. Synthesis proceeds along a path where neutron capture and β-decay compete, much more like a traditional s-process path, albeit at a significantly higher neutron density, over a much shorter time, and farther from stability.

When we combine the observations that (1) individual neutron capture rates impact r-process nucleosynthesis outside of NSE with (2) our work demonstrating that S_{2n} anomalies are an indicator of neutron capture cross section changes, we see a specific example of how nucleosynthesis is connected to the behaviour of nuclear structure observables, particularly S_{2n}. Past studies have observed that phase changes which impact S_{2n} move the position of NSE nucleosynthesis (see [15,17], e.g.). If future mass measurements discover a new region of phase transition, then our correlation would predict that the corresponding neutron capture cross sections would also be affected in a way not predicted by current Hauser-Feshbach formalisms. This would be an indicator that this region of abundances warrants additional study, with particular attention to the neutron capture cross sections and the role of non-NSE capture in setting the final abundances.

4 Conclusions

With existing and new radioactive beam experiments, some of the first measurements on new nuclei will be masses and hence new values for S_{2n}. If anomalous (e.g., non-linear) changes in S_{2n}, especially in neutron rich nuclei, are found, the present results suggest that such anomalies could have an appreciable impact on neutron capture cross sections, which could affect calculated r-process abundances, and that our correlation between S_{2n} and the capture cross sections may provide an improved way to estimate these effects.

Of course, whether this would be visible in the overall abundances would need to be considered in each case.

Acknowledgements A.C. was supported by the US Department of Energy through the Los Alamos National Laboratory by the Laboratory Directed Research and Development program under project number 20190021DR. Los Alamos National Laboratory is operated by Triad National Security, LLC, for the National Nuclear Security Administration of U.S. Department of Energy (Contract No. 89233218CNA000001). R.B.C. acknowledges support by the Max-Planck-Partner group.

Data Availability Statement Data will be made available on reasonable request. [Author's comment: The datasets generated during and/or analysed during the current study are available from the corresponding author on reasonable request.]

Code Availability Statement This manuscript has no associated code/software. [Author's comment: Code/Software sharing not applicable to

this article as no code/software was generated or analysed during the current study.]

References

1. A. Couture, R.F. Casten, R.B. Cakirli, Phys. Rev. C **96**, 061601(R) (2017)
2. A. Couture, R.F. Casten, R.B. Cakirli, Phys. Rev. C **104**, 054608 (2021)
3. M. Wang, G. Audi, F.G. Kondev, W.J. Huang, S. Naimi, X. Xu, Chin. Phys. C **41**, 030003 (2017)
4. F. Iachello, A. Arima, *The Interacting Boson Model* (Cambridge University Press, Cambridge, 1987), pp.113–115
5. I. Dillmann, R. Plag, F. Käppeler, T. Rauscher, In: EFNUDAT Fast Neutrons: Scientific Workshop on Neutron Measurements,Theory, and Applications, edited by F.-J. Hambsch (Publications Office of the European Union, 2010) [http://www.kadonis.org]
6. T. Rauscher, F.-K. Thielemann, Atomic Data and Nuclear Data Tables **79**, 47 (2001)
7. R. Mumpower, R. Surman, G.C. McLaughlin, A. Aprahamian, Progress in Particle and Nuclear Physics **86**, 86–126 (2016)
8. A. Koning, S. Hilaire, M. Duijvestijn [www.talys.eu]
9. E. Margaret Burbidge, G.R. Burbidge, A. Fowler William, F. Hoyle, Rev. of Mod. Phys. **29**, 547 (1957)
10. A.G.W. Cameron, Annual Review of Nuclear and Particle Science **8**, 299 (1958)
11. E. Hans Suess, C. Harold Urey, Rev. Mod. Phys. **28**, 53 (1956)
12. George Wallerstein, Icko Iben, Peter Parker, Ann Merchant Boesgaard, Gerald M. Hale, Arthur E. Champagne, Charles A. Barnes, Franz Käppeler, Verne V. Smith, Robert D. Hoffman, Frank X. Timmes, Chris Sneden, Richard N. Boyd, Bradley S. Meyer, David L. Lambert, Rev. Mod. Phys. **69**, 995 (1997)
13. A.G.W. Cameron, J.J. Cowan, J.W. Truran, Astrophys. Space Sci. **91**(2), 235 (1983)
14. S. Goriely, M. Arnould, Astron. Astrophys. **312**, 327 (1996)
15. Rebecca Surman, Jonathan Engel, Jonathan R. Bennett, Bradley S. Meyer, Phys. Rev. Lett. **79**, 1809 (1997)
16. R. Surman, J. Engel, Phys. Rev. C **64**, 035801 (2001)
17. A. Arcones, G. Martínez-Pinedo, Phys. Rev. C **83**, 045809 (2011)
18. R. Surman, R.J. Beun, G.C. McLaughlin, W.R. Hix, Phys. Rev, C. **79**, 045809 (2009)
19. K. Farouqi, K.-L. Kratz, B. Pfeiffer, T. Rauscher, F.-K. Thielemann, J.W. Truran, The Astrophysical Journal **712**, 1359 (2010)
20. Matthew R. Mumpower, Gail C. McLaughlin, Rebecca Surman, Phys. Rev. C **86**, 035803 (2012)